Available online at www.sciencedirect.com

ScienceDirect

Procedia CIRP 94 (2020) 834–839

www.elsevier.com/locate/procedia

11th CIRP Conference on Photonic Technologies [LANE 2020] on September 7-10, 2020

Production of chip breakers on cemented carbide tools using laser ablation

Berend Denkena[a], Alexander Krödel[a], Lars Ellersiek[a], Marita Murrenhoff[a]*

[a]*Institute of Production Engineering and Machine Tools (IFW), Leibniz Universität Hannover, An der Universität 2, 30823 Garbsen, Germany*

* Corresponding author. Tel.: +49 (0)511 762 18348; fax: +49 (0)511 762 5115. *E-mail address:* murrenhoff@ifw.uni-hannover.de

Abstract

Chip breakers are essential for achieving reproducible and safe turning processes. In case of cemented carbide tools with standard ISO geometries, they are manufactured by form pressing before sintering. In form turning applications with individual tool geometries, chip breakers are typically avoided, because they require an additional and resource intensive grinding process. An alternative preparation strategy for chip breakers is laser ablation. In this paper, the influence of pulse fluence, areal fluence and pulse duration (pico- and nanosecond regime) on ablation mechanisms of cemented carbide tools is investigated. Different ablation mechanisms between pico- and nanosecond-lasers could be detected. Furthermore, a suitable laser ablation strategy using ns-laser is applied to create a chip breaker. Turning investigations showed distinct shorter chips when machining with modified tools.

Keywords: pulsed laser ablation; cemented carbide; form turning tools; chip breakers; ultra-short-pulsed lasers

1. Introduction

Cemented carbide tools are of enormous importance in turning. Tools made of cemented carbide account for 53 % of the worldwide turnover for cutting tools [1]. The production of turning tools is done conventionally by pressing and sintering the inserts. Thereafter, a grinding process is carried out. Normally, chip breakers are inserted into the rake face during pressing. This causes a higher chip curl and a faster chip breakage. Thus, damage on the workpiece due to long chips is prevented and the process reliability is increased [2]. In case of form turning tools, however, the geometry has to be adapted after sintering to the specific process, so that the introduction of chip grooves is not possible during pressing. Laser ablation is an alternative method of creating chip breakers. To obtain suitable laser processes, knowledge about the influence of laser processing on the properties of the cemented carbide is required.

For laser processing of cutting material, mainly pulsed lasers in a pulse duration range between 150 fs and 30 µs in the infrared wavelength range are used [3,4]. The laser process can be characterized by the single pulse fluence

$$F_p = \frac{E_p}{\pi \cdot (\frac{d_f}{2})^2}$$

with

$$E_p = \frac{P_m}{f_p}$$

and areal fluence

$$F_A = \frac{E_p}{PD \cdot TD} ,$$

where f_p is the pulse frequency, P_m the averaged power, d_f the focus diameter and E_p the pulse energy [4,5,6]. A Gaussian energy profile is assumed, whereby the diameter d_f is given at $1/e^2$ (~ 13.5 %) of the energy of the beam centre. It has to be mentioned that the pulse energy E_p depends on the position within the focus diameter. The energy distribution within the

10.1016/j.procir.2020.09.114

laser spot can be approximated by a Gaussian distribution (Fig. 1). The laser power P_m is averaged over time. The peak power P_p can be calculated by

$$P_p = \frac{E_p}{\tau_p}$$

with τ_p as pulse length. Furthermore, *PD* and *TD* are the pulse distance and track distance, respectively, as pictured in Fig. 1. To achieve a uniform surface, TD is commonly set equal to PD.

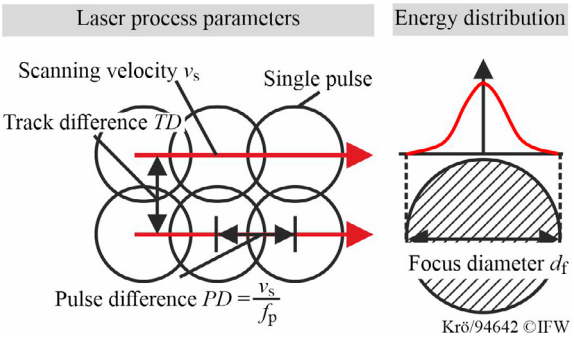

Fig. 1. Laser process definitions

There are already several studies on the laser ablation of cemented carbides, which focus in particular on the preparation of the cutting edge rounding [7,8], the production of micro milling tools [9,10] and micro texturing of cutting tools [3,11]. In [7], the relationship between areal fluence F_A of a ns-laser and ablation efficiency as well as arithmetic mean roughness *Sa* is examined. The ablation efficiency initially increases with increasing fluence, since the energy is not sufficient to sublimate the material completely. However, a further increase of F_A leads to the point that the energy required for sublimation is exceeded and the excess energy is transported into deeper material layers by heat conduction. As a result, material is melted, which results in reduced ablation efficiency and increased roughness. The carbide grade was also varied in the investigations. Five types of carbide with an average grain size between 1 and 2.3 µm and a cobalt content between 6 and 10 % were used. The results show that the carbide grade has no significant influence on the ablation efficiency and the arithmetic mean roughness value Sa. Liu et al. showed that the melting caused by the laser processing leads to phase changes and thus subcarbide phases can arise [11]. Due to the reduction in hardness, the subcarbide phases have a negative impact on the application behavior of the tools [8]. Heating of the surrounding material can be largely avoided with pico- and femtosecond lasers [8]. Processing using ultra-short pulse lasers offers advantages in particular when a large variety of shapes and a low mechanical and thermal load on the object to be processed are required. It was found in [12, 13], that laser material processing results in a modification of the surface topography and hardness. Due to the lower coefficient of thermal conductivity of cobalt compared to tungsten, cobalt melts and evaporates earlier, as well as staggered solidification of both phases, especially with long-pulsed nanosecond lasers. In [9], a dependency between incidence angle, ablation threshold and penetration depth was shown for an ultra-short pulsed laser. In this paper, different ablation mechanisms on cemented carbide tools using ns- and ps-laser are investigated. Basic research on the ablation behavior of laser-prepared cemented carbide surfaces and its material-analytical consideration for the application of chip breaker production has not been carried out to this extent so far. Based on the results, suitable laser parameters are applied to create a chip breaker on a turning tool. Finally, the performance of the prepared tool is compared to a reference tool without chip breaker. The targeted application of laser ablation for the production of chip formers has not been the subject of scientific investigations at present.

2. Experimental Setup

In these investigations, form turning tools (Iscar XNUW 2006-05 IC54) with grain size 1.8 µm were used. The chemical composition on tool surface measured by EDX, is given in Table 1.

Table 1. Chemical composition of unprepared cemented carbide tools

Element	W	C	Co	O	Ti
wt%	83.6	5.2	9.1	1.6	0.5

Laser investigations are performed using a DMG Sauer Lasertec 40 machine tool with pulse length $\tau_p = 70$ ns and an EWAG Laser Line Ultra Piko machine tool with pulse length $\tau_p = 15$ ps. The wavelength of both lasers is $\lambda = 1{,}064$ nm and the beam quality is $M^2 < 1.5$. In addition, both laser machines use scan heads type intelliSCANse from SCANLAB with F-theta lenses from Linos and a focal length of 100 mm. The EWAG Laser Line Ultra Piko has a maximum averaged power $P_m = 50$ W and a focus diameter $d_f = 25$ µm. For the investigations a constant repetition rate $f_p = 200$ kHz, varying average laser power $P_m = 5 – 25$ W and varying scan velocity $v_s = 1{,}000 – 2{,}000$ mm/s were chosen. This corresponds to a pulse energy $E_p = 25 – 125$ µJ and a peak power $P_p = 1.7 – 8.3$ MW. Focus diameter and laser power are based on manufacturer specifications.

The DMG Sauer Lasertec 40 has a maximum averaged power $P_m = 12$ W and a focus diameter $d_f = 40$ µm. For the investigations a constant repetition rate $f_p = 50$ kHz, varying average laser power $P_m = 4 – 12$ W and varying scan velocity $v_s = 300 – 1{,}500$ mm/s were chosen. This corresponds to a pulse energy $E_p = 80 – 240$ µJ and a peak power $P_p = 1.1 – 3.4$ kW. The focus diameter is based on manufacturer specifications, while the laser power was measured with a thermographic measuring instrument Coherent FieldMax PM30. Laser prepared tools were analyzed using a confocal roughness tester Confovis Duo Vario, a Zeiss EVO 60 XVP Scanning Electron Microscope (SEM) and a GE XRD 3003 ETA X-ray diffractometer. All experiments were performed once. Repetition tests are planned in future investigations. However, a high repetition accuracy is expected for the preparation of cutting materials [4,7]. Turning experiments were performed on a CNC lathe Gildemeister CTX 520 linear. 16MnCr5 was machined in orthogonal turning investigations using a tool without chip breaker and a tool with chip breaker created by the ns-laser. The tools were coated with a PVD TiAlN coating after the laser process. Cutting speed, feed and

depth of cut were chosen as v_c = 130 m/min, f = 0.15 mm and a_p = 5 mm, respectively.

3. Laser ablation

3.1. Nanosecond laser

Figure 2 shows the measured roughness of specimens prepared with ns-laser with varying pulse fluence F_P and areal fluence F_A. It can be seen that the highest areal fluence results in the highest roughness. The lowest surface roughness can be achieved for F_A = 13.3 – 177.4 J/mm². A further decrease of F_A results in an increasing roughness. Thus, it can be concluded that the preparation with low, medium and high areal fluences are characterized by different ablation mechanisms. To investigate the underlying effects in more detail, SEM images, EDX measurements and residual stress measurements were carried out for chosen specimens. SEM images and the resulting EDX measurements are shown in Fig. 3. For highest F_A, recrystallized Co-binder material is visible on the surface and a high cobalt content was measured. The material ablation is characterized by melt removal. With decreasing F_A, the recrystallized Co-binder on the surface can be reduced and the ablation depth is slightly decreased. Apparently the energy input is too high, resulting in the center of the laser beam penetrating deep into the carbide. This causes the WC and the Co-binder to become molten but the Co-binder cannot sublimate properly from the resulting melt hollows. As an effect, the co-binder recrystallizes on the surface. Therefore, using low track and pulse distances leads to high number of pulses per area and greater areas of recrystallized Co-binder. Depending on the scan velocity v_s, a geometric pulse overlap of 25 – 85 % was used. For low areal fluences, the resulting surface is more regular and the change in the chemical composition is distinctively smaller. However, the formation of grooves and a melted surface structure are visible, indicating that the energy required for sublimation is below the optimum level. The low energy generates these melting effects, because only slightly above the threshold fluence is operated.

Figure 4 shows an XRD phase diagram and the measured residual stresses of the laser prepared specimens. For reasons of clarity, the x-axis is limited to angles 2θ = 35-60°. Thereby,

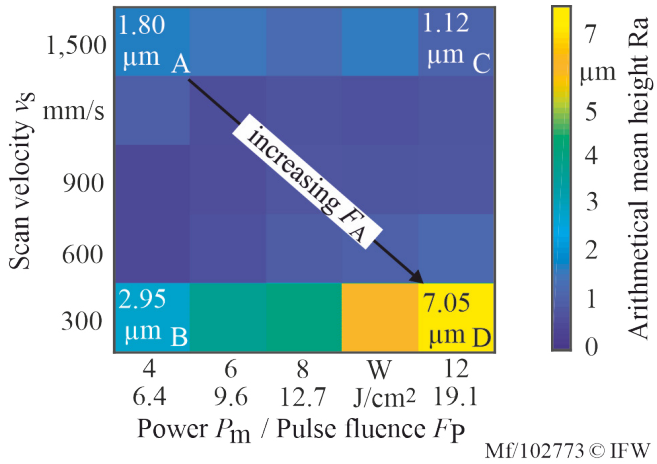

Fig. 2. Resulting surface roughness for different ns-laser parameters

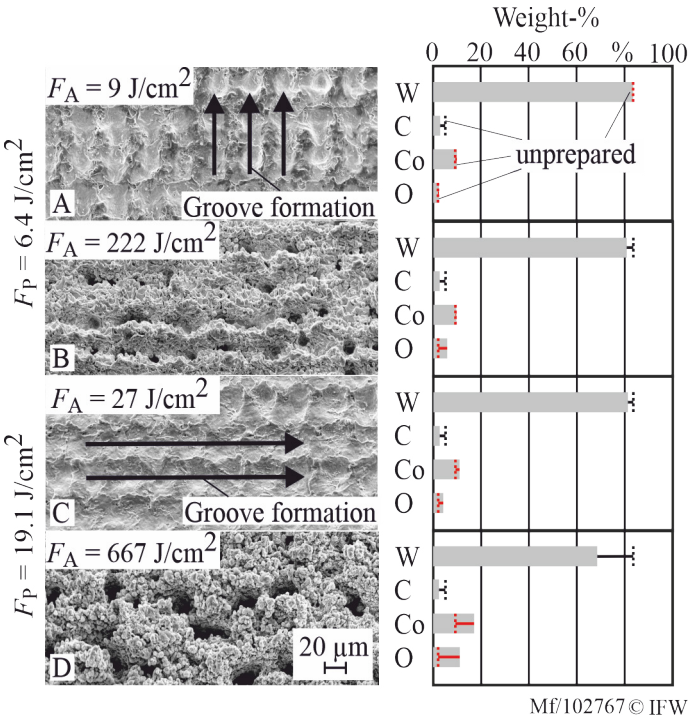

Fig. 3. SEM images and EDX measurements of different specimens prepared with ns-laser

the formation of W_2C can be identified, which is especially evident for high areal fluences F_A, i.e. with increased heat input. Furthermore, WC_{1-x} forms on all laser machined surfaces. The residual stresses were carried out in five repeated measurements with Cu radiation and an information depth of $z_0 \approx 1.7$ µm at the lattice plane WC300. Due to the high energy input in the samples with the higher areal fluences F_A, the lattice plane WC300 was no longer present. In addition, it was

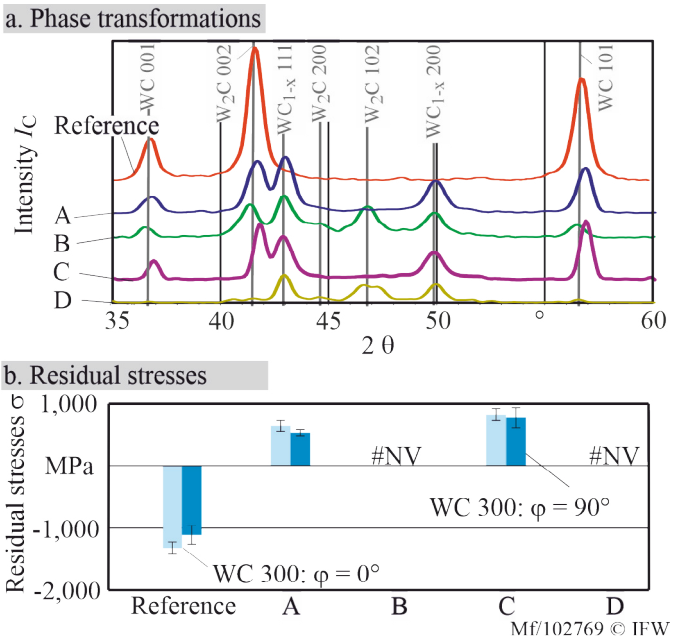

Fig. 4. a. Phase transformations and b. residual stresses for chosen specimens prepared with ns-laser A: F_P = 6.4 J/cm², F_A = 9 J/cm², B: F_P = 6.4 J/cm², F_A = 222 J/cm², C: F_P = 19.1 J/cm², F_A = 27 J/cm², D: F_P = 19.1 J/cm², F_A = 667 J/cm²

found out for sample D with the highest areal fluence that WC101 is the only present WC lattice plane, which has a very low intensity. Therefore no residual stresses could be determined for samples B and D using this measuring method. Furthermore, residual stress measurements with Co radiation and an information depth of ~ 0.7 µm showed an increased residual compressive stress in samples B and D, which is due to the fact that the subcarbide W_2C has formed with a considerably larger cell volume compared to WC. The resulting structural distortions generate the detected residual compressive stresses. From the results presented it can be concluded that a favourable removal behaviour with regard to surface roughness could be achieved at areal fluences F_A = 13.3 - 17.4 J/mm². However, the formation of subcarbides occurred with all laser strategies considered.

3.2. Picosecond laser

Figure 5 shows the surface roughness of specimens prepared with different laser strategies. Depending on the scan velocity v_s, a geometric pulse overlap of 60 – 80 % was used. For low pulse fluences F_P = 5.1 – 10.2 J/cm², the resulting surface roughness is comparatively small. Some additional investigations with pulse fluences down to F_P = 2.6 J/cm² also indicate a good ablation behavior for lower pulse fluences, which can be attributed to the fact that plasma formation is avoided due to the short pulse length. Therefore, large part of the energy can be transferred into the material. High F_P and F_A result in a significantly higher surface roughness because the optimum energy required for sublimation is exceeded.

Due to the respective machine characteristics of the nanosecond and picosecond laser, the power within one pulse of the picosecond laser is significantly higher than that of the nanosecond laser. As a result, the energy used is far above the ablation and sublimation threshold. Accordingly, a different ablation behavior is obvious for the picosecond laser used compared to the nanosecond laser.

Analogous to the investigations with ns-laser, detailed investigations were carried out for four different specimens. Figure 6 shows SEM images and the chemical composition of laser prepared specimens. For the low pulse fluence F_P = 5.1 J/cm², a low surface roughness can be achieved. No

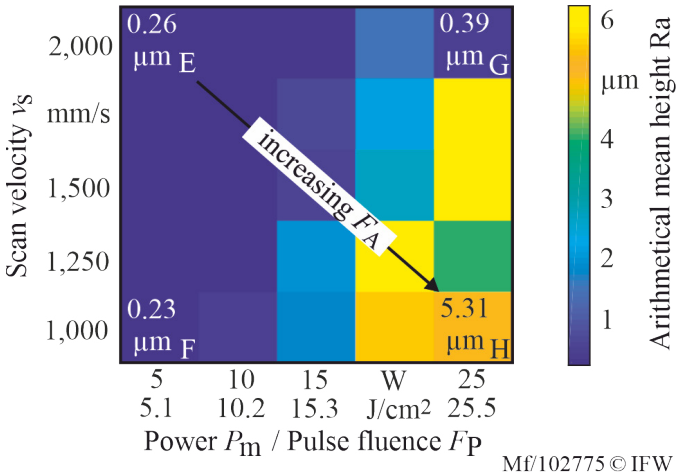

Fig. 5. Resulting surface roughness for different ps-laser parameters

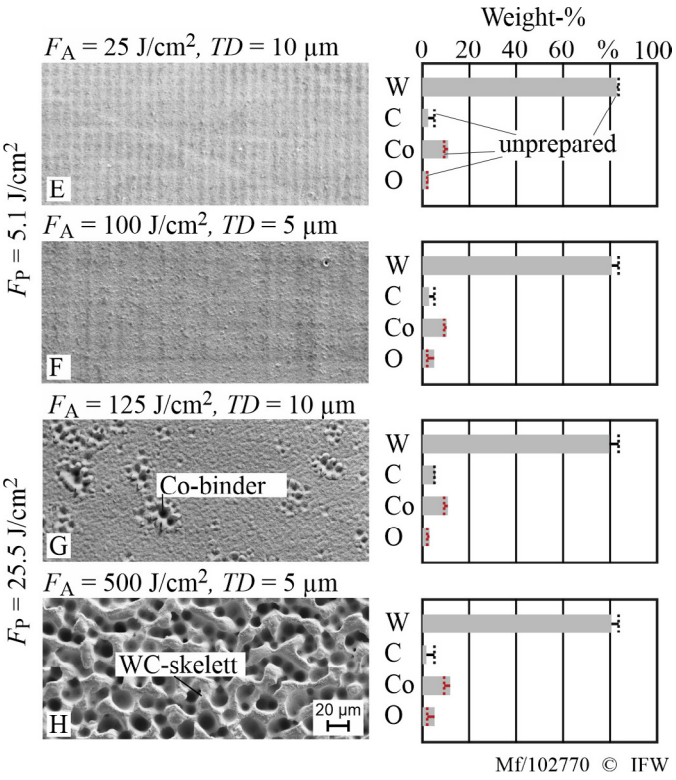

Fig. 6. SEM images and EDX measurements of chosen specimens prepared with ps-laser

surface defects are visible on the SEM images. For high pulse fluence F_P and low areal fluence F_A, small areas of melted cobalt binder are visible on the surface as suggested by EDX mapping. An increase of F_A results in a removal of the cobalt binder inbetween WC grains. This can be explained by the fact that the energy transferred due to heat conduction is sufficient

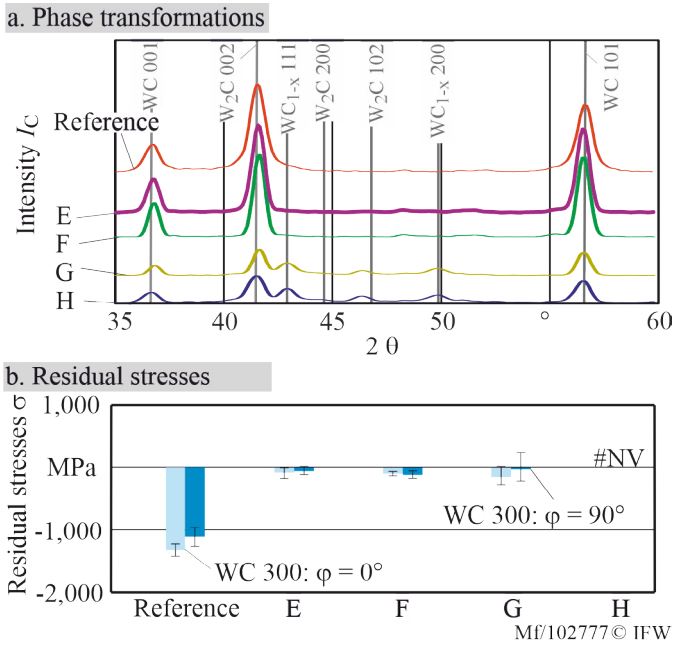

Fig. 7. a. Phase transformations and b. residual stresses for chosen specimens prepared with ps-laser E: F_P = 5.1 J/cm², F_A = 25 J/cm², F: F_P = 5.1 J/cm², F_A = 100 J/cm², G: F_P = 25.5 J/cm², F_A = 125 J/cm², H: F_P = 25.5 J/cm², F_A = 500 J/cm²

to remove the cobalt, which has a lower thermal stability than tungsten carbide. However, in terms of chemical composition, similar effects occur on all specimens. While tungsten and carbon content are reduced, the cobalt and oxygen content are increased. A possible explanation is the diffusion of heated cobalt to the surface as stated in [14]. This effect increases with increasing heat input.

XRD scans and measured residual stresses are shown in Fig. 7. It can be seen that subcarbides W_2C and WC_{1-x} only form for the specimens prepared with high pulse Fluence F_P. Therefore, in contrast to the preparation with ns-laser, the formation of subcarbides can be avoided for certain laser strategies due to the short heat input. Tensile residual stresses were measured five times for all laser-prepared samples. Obviously, the effect of thermally induced tensile residual stresses is lower due to the ps-laser, since the residual compressive stresses were measured for the most part. The machined surfaces can therefore be considered approximately stress-free. However, as with the ns-laser, the mesh level WC300 was no longer present in sample H due to the increased thermal input.

Finally, it can be stated that pulse fluences $F_P = 5.1 – 10.2$ J/cm^2 lead to a beneficial ablation behavior. In this parameter range, the formation of subcarbides can be avoided and a low surface roughness can be achieved.

4. Form turning investigations

To evaluate the potential of chip breakers on form turning tools, machining investigations were carried out. For this purpose, blanks for form turning inserts were machined with a ns-laser. Although the cemented carbide was influenced significantly more when processing with ns-laser compared to ps-laser, the ns-laser was used in this investigations due the high industrial relevance of that laser type, e.g. in preparation of diamond tools.

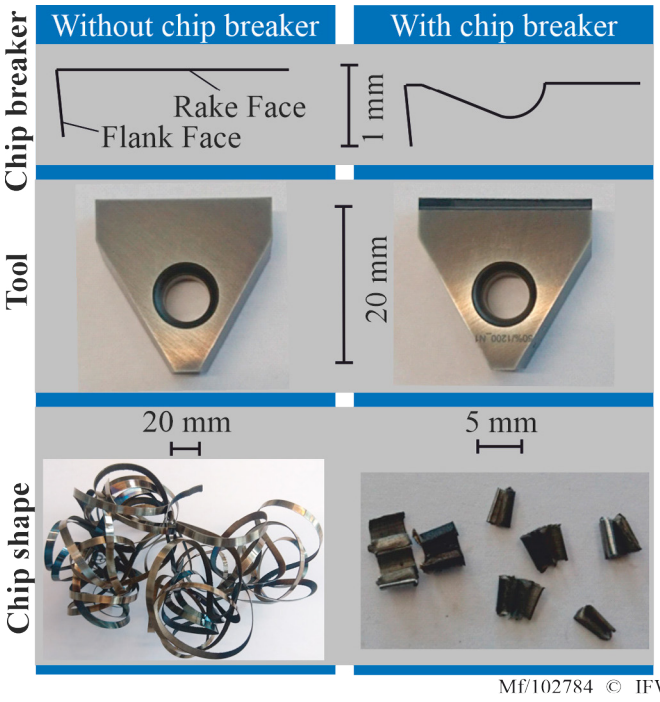

Fig. 8. Dependence of chip formation on the chip former for AISI 5115. ns-laser, laser preparation: $P_m = 6$ W, $f_p = 50$ kHz, $v_s = 1{,}200$ mm/s, orthogonal cutting: $f = 0.15$ mm, $v_c = 130$ m/min, $a_p = 5$ mm.

For the laser preparation, a power of $P_m = 6$ W, a repetition rate $f_p = 50$ kHz and a scanning speed $v_s = 1{,}200$ mm/s were chosen and a defined chip breaker geometry was ablated. The previous investigations indicate a good ablation behavior for this laser strategy. For orthogonal cutting, the material AISI 5115 was machined with a feed rate $f = 0.15$ mm, a depth of cut $a_p = 5$ mm and a cutting speed of $v_c = 130$ m/min. An unprepared form turning tool without chip breaker was used as a reference. The blanks for profile grooving were initially used without an inserted form geometry.

Figure 8 shows the chip breaker geometry, the used tools and the produced chips. The chip breaker geometry is characterized by a flat slope of the contour and a subsequent steep ascent. This leads to a strong curvature of the chips and thus to greater stresses in the chips, which promotes chip breakage. For the reference tool without chip breaker, a snarled chip formed during machining, which was completely wrapped around the machined workpiece. Chip breakage occurred during the application tests with the chip breaker inserted and spiral chip segments have formed. Thus, damage of the workpiece due to an unsuitable chip form can be prevented. Process reliability can be increased by targeted chip breaking and tool wear can be reduced. In addition, an increase in performance can be achieved by using a chip breaker, as it is possible to work in continuous cutting mode without interrupting the cutting process to remove the chips.

5. Conclusions

The investigations carried out result in the following conclusions:

- For ns-lasers with low pulse fluence F_p, the ablation depth is low since the energy is only sufficient for material removal in the center of the laser spot. Therefore, the material is characterized by high roughness and phase transformations.
- The surface prepared with ps-laser has significant improved surface properties and higher ablation depths compared to the ns-laser for low pulse fluence Fp. This can be attributed to the avoidance of plasma formation due to the short pulse duration.
- For the highest pulse fluence, the energy need for sublimation is exceeded and the excess energy is transported deeper into the material, leading to surface defects and tensile residual stresses.
- The chip form can be significantly improved by using laser-prepared chip breakers.

In future investigations, the following research topics are focused:

- To quantify the difference between different laser sources in more detail, additional investigations using a fs-laser are carried out.
- The influence of laser preparation on tool wear, especially when using coated tools, has to be investigated.

- A method for designing chip breakers, e.g. by using Finite-Element simulations, has to be established.
- Furthermore, different chip groove geometries with different laser preparation strategies will be created and compared. In addition, selected form turning tool geometries will be prepared with chip breakers and used in turning investigations.

Acknowledgement

The IGF-project (IGF – 20766 N) of the Research Association (VDW – Forschungsinstitut e.V.) was supported by the AiF within the program for the promotion of industrial research (IGF) from the Federal Ministry of Economy and Energy due to a decision of the German Bundestag. The authors would like to thank Iscar Germany GmbH for providing the cutting tools, the WOLF coating & parts GmbH for coating the tools and EWAG AG for the use of the laser machine.

References

[1] Bobzin K. High-performance coatings for cutting tools. CIRP Journal of Manufacturing Science and Technology, Vol. 18, p. 1–9, (2017)
[2] Buchkremer S. Predictive Tool and Process Design for Efficient Chip Control in Metal Cutting, PhD-Thesis, RWTH Aachen, Germany, (2015)
[3] Fang S, Soldera F, Rosenkranz A, Herrmann T, Bähre D, Llanes L, Mücklich F. Soldera. Microstructural and Metallurgical Assessment of the Laser-Patterned Cemented Tungsten Carbide (WC-CoNi), 46th SME North American Manufacturing Research Conference, Texas, USA, (2018)
[4] Pacella M. Pulsed laser ablation of ultra-hard structures: generation of tolerant freeform surfaces for advanced machining applications, PhD-thesis, University of Nottingham, United Kingdom, (2014)
[5] Denkena B, Krödel A, Grove T. On the pulsed laser ablation of polycrystalline cubic boron nitride—Influence of pulse duration and material properties on ablation characteristics, Journal of Laser Applications 31, (2019)
[6] Daniel C, Ostendorf S, Hallmann S, Emmelmann C. Picosecond laser processing of polycrystalline cubic boron nitride — A method to examine the ablation behavior of a high cubic boron nitride content grade material, Journal of Laser Applications 28, (2016)
[7] Gutwein S, Kirsch B, Herrmann T, Derouach H, Aurich JC. Kurzpulslaserbearbeitung unterschiedlicher Hartmetallsorten, ZWF – Zeitschrift für wirtschaftlichen Fabrikbetrieb Vol. 113, p. 453-457, (2018)
[8] Bouzakis KD, et al. Effect of HM substrates' cutting edge roundness manufactured by laser machining and micro-blasting on the coated tools' cutting performance, CIRP Journal of Manufacturing Science and Technology, Vol. 18, p. 188-197, (2017)
[9] Hajri M, Börner P, Wegener K: An industry-relevant method to determine material-specific parameters for ultra-short pulsed laser ablation of cemented carbide, CIRP Conference on Photonic Technologies, Fuerth, Germany, (2018)